Topographic Component (Parallel Factor) Analysis of Multichannel Evoked Potentials: Practical Issues in Trilinear Spatiotemporal Decomposition

Aaron S. Field and Daniel Graupe

Summary: We describe a substantive application of the trilinear topographic components /parallel factors model (TC/PARAFAC, due to Möcks/Harshman) to the decomposition of multichannel evoked potentials (MEP's). We provide practical guidelines and procedures for applying PARAFAC methodology to MEP decomposition. Specifically, we apply techniques of data preprocessing, orthogonality constraints, and validation of solutions in a complete TC analysis, for the first time using actual MEP data. The TC model is shown to be superior to the traditional bilinear principal components model in terms of data reduction, confirming the advantage of the TC model's added assumptions. The model is then shown to provide a unique spatiotemporal decomposition that is reproducible in different subject groups. The components are shown to be consistent with spatial/temporal features evident in the data, except for an artificial component resulting from latency jitter. Subject scores on this component are shown to reflect peak latencies in the data, suggesting a new aspect to statistical analyses based on subject scores. In general, the results support the conclusion that the TC model is a promising alternative to principal components for data reduction and analysis of MEP's.

Key words: Evoked potentials; Principal components; Topographic components; Spatiotemporal analysis; Decomposition.

Introduction

A fundamental problem in spatiotemporal analysis of multichannel evoked potentials (MEP's) is that of data reduction, made necessary by the typically large quantities of data available for study. It is not our intent to distinguish evoked potentials from event-related potentials in general; this paper is relevant to waveforms time-locked to any event and sampled over any epoch, and to single-trial as well as averaged waveforms. One of the most popular approaches to the evoked potential (EP) data reduction problem has been the method of principal component analysis (PCA) (see Glaser and Ruchkin 1976; Donchin and Heffley 1978). In a typical application of PCA, a set of EP waveforms is decomposed into a small number of "component" waveforms, which combine linearly to represent each data waveform. PCA can also be applied in the spatial domain, such that a set of topographic maps is decomposed into a small number of component maps (e.g., Skrandies and Lehmann 1982; Skrandies 1989). Regardless of which approach is taken, problems inherent in the PCA method have made its use in EP analysis somewhat controversial (e.g., Wood and McCarthy 1984; Möcks and Verleger 1986).

The most serious criticism of PCA concerns the rotational indeterminacy of the components. Due to the bilinear form of the model underlying PCA, linear transformations (rotations) can be used to obtain infinitely many different sets of components that provide equivalent representations of the data in the least-squares sense. Another criticism concerns the mutual orthogonality that is the nature of principal components. It is unreasonable to expect the activities of individual neural "generators" to be mutually orthogonal - thus the physiologic reality of any set of principal components is questionable.

The drawbacks inherent in PCA motivated the development of a new model for EP decomposition. The

Department of Electrical Engineering and Computer Science and Department of Bioengineering, University of Illinois at Chicago.

Accepted for publication: March 15, 1991.

This paper contains portions of the first author's dissertation, submitted in partial fulfillment of the requirements for the Ph.D. degree, Department of Bioengineering, University of Illinois at Chicago. The authors are indebted to G. Raviv of Bio-logic Systems Corp., Mundelein, Illinois, USA, for providing proprietary data and topographic mapping software used in this research; R. A. Harshman and M. E. Lundy of Scientific Software Associates, London, Ontario, Canada, for advising on the use of the PARAFAC analysis package; the Computer Center of the University of Illinois at Chicago for providing computational and plotting facilities; J. Kripal for helping to collect the data; and M. Field for assisting with the manuscript. They also thank R. A. Harshman and anonymous reviewers for their comments on an earlier draft of the paper.

Correspondence and reprint requests should be addressed to Daniel Graupe, The University of Illinois at Chicago, Department of Electrical Engineering and Computer Science (M/C 154), Box 4348, Chicago, Illinois, 60680, USA.

topographic components (TC) model (Möcks 1988a, 1988b) solves the problem of indeterminancy by means of a *trilinear* decomposition that is theoretically unique. That is, once identified, the components are not subject to transformation (rotation). Moreover, the components are not orthogonal by definition. In addition to these desirable properties, the TC model gives equal importance to the spatial and temporal features of the data, providing data reduction in both domains, and provides an explicit basis for comparisons between subjects.

In developing the TC model, Möcks independently rediscovered the mathematically identical models known as PARAFAC, for PARAllel FACtors (Harshman 1970; Harshman and Lundy 1984a, 1984b), and CANDECOMP, for CANonical DECOMPosition (Carroll and Chang 1970; Carroll and Pruzansky 1984). These models are used for analysis of three- and higher-way data arrays, mainly in psychology research, but to our knowledge have not been applied to dynamic signals such as EP's. Möcks' TC model can be considered a special interpretation of the PARAFAC – CANDECOMP model (for convenience, simply PARAFAC), which is generic in the sense that it is not intended for data from any particular source. Möcks (1988b) provided justification for the model in the context of EP analysis, based on biophysical considerations. With this understood we refer to the model as PARAFAC and TC interchangeably.

Along with the TC model's advantages over PCA comes a less straightforward procedure for performing the decomposition and interpreting the results. Harshman and Lundy (1984a, 1984b, Harshman 1984, and Harshman and DeSarbo 1984) have made it clear that proper use of the PARAFAC model requires a number of decisions, e.g., regarding data preprocessing, optional orthogonality constraints, model order, and validation of solutions. Such decisions must be made appropriately for a given data set, often with little or no a priori knowledge available as a basis. Therefore, the merits and drawbacks of the TC model with respect to EP analysis are not clear or predictable from the basic theory as in Möcks (1988a, 1988b).

This paper unites the theory of the TC model with the methodology of PARAFAC analysis, using for the first time actual MEP data. The significance of this contribution is pointed to by the fact that (1) a practical method of analysis for MEP's (or indeed for any multichannel dynamic signals), based on the TC or PARAFAC model, has never been developed; (2) the model will be of little use until practical guidelines on how to apply it appropriately to MEP's are established; and (3) it has never been demonstrated that the TC model is even appropriate for MEP's.

We present the complete TC analysis of an actual MEP waveform set, using the methodology of PARAFAC. Our purpose is as follows: (1) demonstrate the methods and results associated with the TC model as applied to MEP's; (2) offer a suggested approach for potential users to the decision-making process required for successful application of the model to MEP's; (3) where possible, establish theoretical or empirical guidelines for appropriate application of the TC model to MEP's; (4) evaluate the appropriateness of the TC model for MEP's, particularly as compared to traditional principal components; and (5) obtain a unique and meaningful spatiotemporal decomposition of our MEP data and evaluate its interpretability. It is hoped that this paper will provide a helpful "initiation" to the practical aspects of TC analysis for the reader who is familiar with PCA and who may be interested in an alternative approach to the problem of MEP decomposition.

The Topographic Components Model

Model Definition and Terminology

The TC model is defined to represent a set of time-sampled EP waveforms recorded using multiple scalp locations from a group of subjects. Following Möcks (1988a), let $x\,(i,l,t)$ denote potential as a function of subjects $i = 1,...,I$; scalp locations $l = 1,...,L$; and sample times $t = 1,...,T$. These data are modelled by the following trilinear sum:

$$x\,(i,l,t\,) \approx \sum_{k=1}^{N} a_k\,(i\,)\,b_k\,(l\,)\,c_k\,(t\,) \qquad (1)$$

where $c_k(t)$ is the kth component waveform, common to all subjects and locations; $b_k(l)$ is the kth component distribution, common to all subjects and sample times; and $a_k(i)$ is the set of weighting coefficients that reflect the contributions made by the kth component (waveform and distribution together), to the data observed for each subject. With weak assumptions (see Möcks [1988b] for a simple proof, and Harshman and Lundy [1984b] for a full discussion) model (1) provides a theoretically unique decomposition, up to trivial permutation, scaling, and sign changes. Furthermore, (1) provides data reduction in both spatial and temporal domains, as well as an explicit parameterization of the inter-individual variations within a subject sample.

As an aside, note that for a single subject, the three-way data array $x\,(i,l,t)$ reduces to a two-way matrix, and the trilinear model (1) reduces to the bilinear form that is characteristic of PCA. Singular value decompositon (SVD) has been applied to EEG/EP's by Harner (1990). Like PCA, SVD effects the decomposition of a two-way

data matrix. In fact, the models underlying SVD and PCA have the same bilinear form, and the two decompositions are essentially equivalent. Thus, SVD has the same disadvantages as PCA, the most important being rotational indeterminacy.

It is convenient to refer to the functions c_k (t) as "temporal components", the distributions b_k (l) as "spatial components" and the weighting coefficients a_k (i) as "subject scores". Note, however, that the model is symmetric in the three domains (or modes), i.e., although specific interpretations are attatched to the a-, b-, and c-parameters, they are mathematically equivalent. Using PARAFAC terminology, the parameters in a given mode will occasionally be referred to as "loadings". The term "component" will be used in the generic sense when the meaning is understood, rather than the equivalent PARAFAC term "factor".

Parameter Estimation and Uniqueness

Parameter estimation for trilinear models like (1), as well as for other multilinear models, is traditionally accomplished by the iterative method of alternating least-squares (ALS - Carroll and Chang 1970). We found the ALS algorithm faster to converge and simpler to compute than the gradient-type method used previously by us (Field and Graupe 1990a). All results for this paper were obtained using the PARAFAC analysis software package (Lundy and Harshman 1985), which employs an ALS estimation algorithm.

Each fit value (measure of goodness-of-fit) reported in this paper is the best of three repeated runs of the estimation algorithm, starting from different random positions as provided by the PARAFAC software. The standard PARAFAC convergence criterion was used: convergence was assumed when no loading changed by more than 0.1% of the root-mean-square (RMS) average loading for the given component in the given mode, from the previous iteration (Lundy and Harshman 1985). When the solution itself was of interest as well as the fit value, uniqueness was verified by comparing solutions among the three runs. In no case was an "odd" solution identified that could not be explained by incomplete convergence (as indicated by a significantly poorer fit) and disregarded. The fit value used is the relative mean-squared error (MSE):

$$MSE \triangleq \frac{\sum_{i,l,t} e^2(i,l,t)}{\sum_{i,l,t} x^2(i,l,t)} \qquad (2)$$

where e (i, l, t) and x (i, l, t) are the error and data values respectively, and $\Sigma_{i,l,t}$ denotes the triple sum $\Sigma^{I}_{i=1}$ $\Sigma^{L}_{l=1}$ $\Sigma^{T}_{t=1}$. It is usually desirable to adopt some conventions for scale, sign, and permutation (sequence) of the model components since these are arbitrary (see, e.g., Field and Graupe 1990a). The conventions used in this paper will be described later.

Preliminary Studies with Visual Evoked Potentials

Data Protocol

The data used for these studies consisted of average pattern-reversal visual EP (PVEP) waveforms, recorded from 30 normal subjects at 8 scalp locations (C3, Cz, C4, P3, Pz, P4, O1 and O2, Int.10-20 System). The stimulus was full-field checkerboard pattern reversal with both eyes open, and averaging was over 200 trials. The waveform baseline convention was zero-potential difference with a linked-mandible reference. The data were recorded at various laboratories and collected by Biologic Systems Corp. (Mundelein, Illinois, USA), for inclusion in a normative PVEP data base. A standardized protocol was used for all recordings (Bio-logic Systems Corp. 1988) and the determination of "normality" for each subject was based on a complete medical history as well as inspection of the data by a clinical neurologist. The waveforms were originally sampled at 1-msec intervals from 0 to 256 msec post-stimulus; however, in order to minimize computations, only every fourth sample was included in the analysis, resulting in sixty-four samples at 4-msec intervals for each waveform. Thus, the three-way data array was 30 subjects × 8 locations × 64 sample times.

Data Preprocessing

Before fitting the TC model, the data must be preprocessed. The importance of preprocessing has been emphasized by Harshman and Lundy (1984a). PARAFAC preprocessing will now be briefly reviewed in the general context, followed by a discussion of the specific considerations that arise with MEP data.

There are basically two ways to preprocess a three-way data array prior to fitting the PARAFAC model: rescaling and centering. Consider first rescaling, which involves multiplying various subsets of the data by constant "scale factors", and is usually done to normalize data mean-squares over the various "levels" of a given mode (e.g., over subjects). This accomplishes two things: (1) It eliminates arbitrary and unwanted variations in scale magnitudes across the various levels, and (2) it assures that the data at all levels will have the same influence over the least-squares-fitted solution. If overall magnitude variations are of interest but the latter result (2) is desired, the model can be fitted to the normalized

data, and then the model parameters scaled back to reflect the original magnitudes present in the data. This is a straightforward procedure that in no way complicates the interpretation of components - see the discussion of "weighted least-squares" by Harshman and Lundy (1984a).

Centering involves subtracting constants-specifically means-from various subsets of the data. This is done to remove constant offsets that are inconsistent with the model, since implicit in the model is the assumption that the data were measured on a scale having a fixed origin, consistent across all levels of each of the three data modes. In the present context, this says that "zero potential" is fixed for all subjects, all locations, and all sample times. Note, this assumption is suspect because potential measurements are relative, i.e., no absolute zero can be defined.

Either rescaling or centering, or both, can be done on any or all of the 3 data modes (A, B, and C). The two operations may interfere with one another, depending on which modes and in what sequence the operations are performed. Therefore, an iterative procedure is sometimes required to achieve the desired combination of centering and rescaling. The various preprocessing options will now be considered in the context of MEP data.

Rescaling of Evoked Potentials Data

Rescaling mode A (subjects) might be used to normalize the data across subjects, in order to correct for arbitrary variations in overall signal strengths due to variations in head size or scalp thickness, for example. This seems desirable, since it is generally not overall signal strengths that are of interest but rather the spatial and temporal dynamics of the data. Rescaling might also be used to normalize the data across locations and sample times, respectively. This, however, would be undesirable. Unlike such variations across subjects, variations in signal strengths from one time or location to another are not arbitrary; rather, they constitute the very information that is of interest.

It was noted above that the data can be normalized across levels of a given mode in order to give the data at each level the same influence in determining the least-squares solution, and then, after fitting the model, the parameters of the rescaled mode(s) can be scaled back to reflect the original magnitudes that were present in the data before rescaling. With regard to EP data, again, this would only be appropriate for mode A (subjects). If we assume noise levels to vary from subject to subject but remain relatively fixed over time and space for each subject, then times or locations that tend to have weaker potentials will be associated with lower signal-to-noise ratios (SNR). This will not necessarily be true with respect to subjects. Stated another way, smaller data values represent less reliable measurements from one time or location to another; however, across subjects, a tendency toward smaller data values may reflect lower levels of both signal and noise. Thus, mode A can be normalized if desired, neglecting whatever unknown differences in SNR there may be between subjects. More reliable data should be allowed accordingly more influence by not normalizing over locations (mode B) or sample times (mode C). By the same token, if one or more channels are known to be noisier in all subjects, rescaling can be used to deemphasize those channels.

Summarizing the rescaling options for multisubject MEP data, normalization of the data to equalize mean-squares is inappropriate over locations (mode B) or sample times (mode C), but is appropriate and desirable over subjects (mode A). If differences in overall signal strengths between subjects is of interest, the A-mode loadings (subject scores) can be scaled back to reflect those differences after fitting the model.

Centering of Evoked Potentials Data

Centering on mode A can be thought of as subtracting out an "average subject" from the data, such that the centered data reflect only how each subject deviates from the average. If one is interested mainly in individual differences among a group of subjects, then emphasizing such differences by centering the subject mode would be appropriate. On the other hand, one might be more interested in a group of subjects as a whole, and wish simply to use the TC model for data reduction on the group. In this case one would fit the model to the uncentered data. (Although uncentered data is inappropriate for the model *per se*, the model *can* fit uncentered data - it is just more difficult.) Finally, note that A-centering is likely to significantly reduce the SNR of the data, particularly for a homogeneous group of subjects.

In centering on mode B, the potential mean over all electrodes is subtracted from the data for each subject and each sample time. This is equivalent to transforming the data to average reference (Offner 1950). Use of the average reference has been advocated as a way to achieve reference-independent data, avoiding problems associated with the relativity of potential measurements and the non-existence of a truly "indifferent" or "inactive" reference electrode (Lehmann 1987, Nunez, 1981).

In centering on mode C the potential mean over time is subtracted from each individual waveform, i.e., the data are transformed to zero-mean baseline. Normally the baseline for each waveform corresponds to zero-potential difference between the recording electrode and the reference. It has been our experience that waveform

means tend to be relatively small, such that centering mode C would be unlikely to have a significant effect on fitting the TC model (certainly as compared to centering modes A or B). Therefore, although it is not inappropriate per se, we have avoided C-mode centering in our work to date.

Summarizing the centering options for multisubject MEP data, A-, B-, and C-mode centering transform the data to deviations from the average subject, average refence, and zero-mean baseline, respectively. A- and/or B-mode centering may or may not be desirable, depending on the goals of a particular analysis. C-mode centering we consider to be both unnatural and unnecessary. Finally, any centering will decrease the SNR of the data to some degree.

Practical Evaluation of Centering Options

Unlike rescaling, centering alters the structure of the data and will therefore affect the ability of the model to fit the data. Therefore, to choose the appropriate centering for our PVEP data, we compared fit-dimensionality curves after (1) no centering, (2) A-mode centering, and (3) B-mode centering. Additional information to aid the choice of centering was obtained by the following Monte Carlo procedure: Three fit-dimensionality curves were obtained by fitting the model to a synthetic data set that was in effect a "partially randomized" version of the actual data set. The synthetic data set matched the actual data set in dimensions (30 × 8 × 64) but consisted of random numbers, adjusted to have the same second-order statistics (means and mean-squares) as the actual data in each of the three modes. Thus, the proportion of the total data-mean-squares contributed by the non-zero means in each mode (i.e., the information that is removed by centering) was the same for the synthetic data as for the actual data. Moreover, these non-zero means constituted the only information in the synthetic data (i.e., if the synthetic data were to be centered on all three modes, they would become 100% noise). This approach, similar to the randomization tests recommended by Harshman and Lundy (1984b), provided a basis for evaluating the extent to which the model (1) fit systematic variation in the data (i.e., information) versus noise, and (2) fit variation associated with the non-zero means versus variation that remained after centering. This is especially important because the different centering operations reduce the SNR of the data to an unpredictable degree.

The synthetic data set $s(i,l,t)$ began as a $30 \times 8 \times 64$ array of standard normal deviates. These data were adjusted to have the same means and mean-squares over all three modes as the actual data $x(i,l,t)$ by repeatedly offsetting (by additive constants) and rescaling the data in each mode until the following equations were satisfied:

$$\sum_{i=1}^{I} s(i,l,t) = \sum_{i=1}^{I} x(i,l,t) \quad \forall\, l,t \tag{3}$$

$$\sum_{l=1}^{L} s(i,l,t) = \sum_{l=1}^{L} x(i,l,t) \quad \forall\, i,t \tag{4}$$

$$\sum_{t=1}^{T} s(i,l,t) = \sum_{t=1}^{T} x(i,l,t) \quad \forall\, i,l \tag{5}$$

$$\sum_{l=1}^{L}\sum_{t=1}^{T} s^2(i,l,t) = \sum_{l=1}^{L}\sum_{t=1}^{T} x^2(i,l,t) \quad \forall\, i \tag{6}$$

$$\sum_{i=1}^{I}\sum_{t=1}^{T} s^2(i,l,t) = \sum_{i=1}^{I}\sum_{t=1}^{T} x^2(i,l,t) \quad \forall\, l \tag{7}$$

$$\sum_{i=1}^{I}\sum_{l=1}^{L} s^2(i,l,t) = \sum_{i=1}^{I}\sum_{l=1}^{L} x^2(i,l,t) \quad \forall\, t \tag{8}$$

where I=30, L=8, T=64 and ∀= "for all" . The resulting data set will be referred to as the "randomized" data set.

The PARAFAC analysis package was used to preprocess the data and fit the TC model. The A-modes of both actual and randomized data sets were rescaled to normalize mean-squares across subjects, as discussed earlier. First- through fifth-order models were fitted, and for each order the best fit among three different runs was noted. The six fit-dimensionality curves are shown in Figure 1. A seventh curve, obtained by fitting pure noise (the randomized data set centered on all three modes), is also plotted for comparison.

Some observations: (1) With no centering, the model fit the actual data only nominally better than it fit the randomized data (curves a vs. d). This suggests that in the actual data, the model fit predominantly that portion of the total mean-squares contributed by the non-zero means, and little beyond that. (2) After A-centering, the MSE's were significantly higher than with no centering, for both the actual and the randomized data (curves b and e vs. a and d, respectively). That removing the A-mode means reduced the goodness-of-fit to such a degree indicates that the A-mode means represented a significant portion of the total data-mean-squares that was explained by the model, despite that such constants

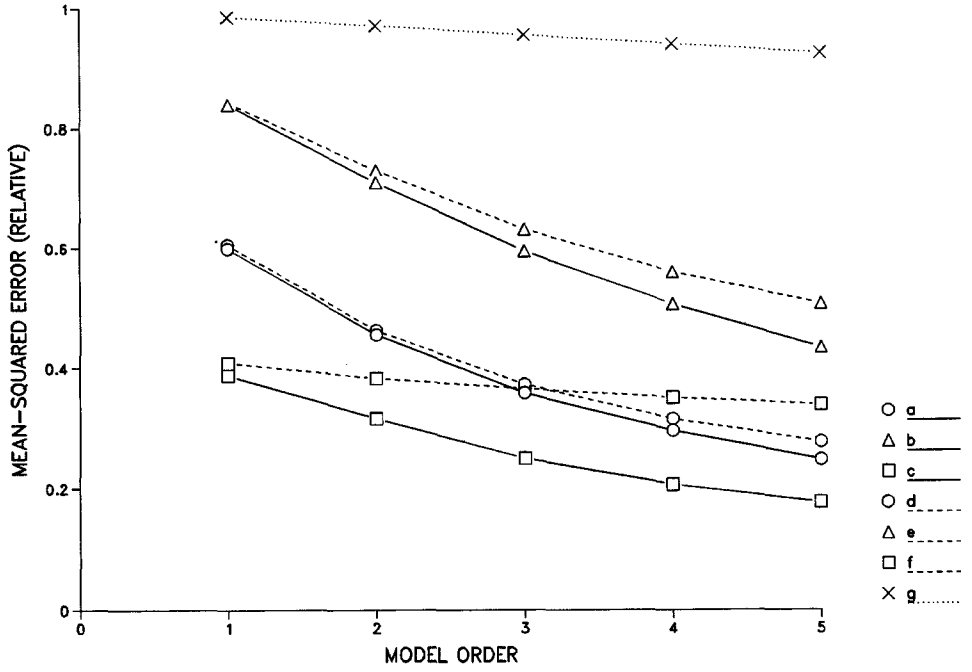

Figure 1. Fit-dimensionality curves show effects of centering. Solid curves: actual data, (a) uncentered, (b) A-centered, (c) B-centered. Dashed curves: randomized data, (d-f) same as (a-c). Dotted curve (g): totally random data, centered on all three modes.

are inconsistent with the model per se. (3) After A-centering, as with no centering, the model fit the actual data only nominally better than it fit the randomized data (curves b vs. e). This suggests that after A-centering, it was primarily the B-mode means that were accounted for by the model (C-mode means were negligible). (4) After B-centering, the model fit the actual data significantly better than it fit the randomized data (curves c vs. f). This confirms that the actual data do in fact show systematic variation, beyond that associated with the non-zero means, which can be explained by the model. (5) The model fit the actual data better after B-centering than with no centering (curves c vs. a). This confirms that B-centering had the desired effect of leaving the data in a form that is more appropriate for the model.

What can be concluded from these results about the centering options? First, from observation (1), some centering of these data will be essential if the model is to represent anything beyond the means in each mode of the data. Second, from the remaining observations, B-centering is a better choice than either A-centering or no centering for these data, giving the lowest MSE's overall: 0.18 at fifth-order (curve c), versus 0.25 with no centering (curve a), and versus 0.43 after A-centering (curve b). B-centering also gave the lowest MSE's relative to the corresponding randomized data: 0.16 absolute difference at fifth-order (curves c vs. f), compared to 0.03 with no centering (curves a vs. d) and 0.07 after A-centering (curves b vs. e).

A-centering appears to have eliminated too much variation in the data that the model is able to explain, i.e., it appears to have significantly reduced the SNR. It is not surprising that the A-mode means account for a large proportion of the total mean-squares: In general, EP waveforms compared between normal subjects appear much more alike than different. In fact, Harshman and Lundy (1984a) noted in their work with other types of (non-dynamic) data that centering the subject mode "... sometimes seems to emphasize those individual differences that are inconsistent with the model..."

It must be emphasized that the above conclusion cannot be generalized to other EP data—for a given data set, all centering options should be considered. Constructing a set of curves like those in Figure 1 is a useful method for examining the effects of different or no centerings prior to analyzing a given data set. Experience with the TC model may eventually reveal particular centerings to be appropriate in certain situations, perhaps obviating the need for a decision on centering when using traditional experimental designs.

Degenerate Solutions and Orthogonality Constraints

Harshman and Lundy (1984a) found that a serious problem with the PARAFAC model is the frequent tendency of the least-squares optimal solution to be "degenerate". They use this term to describe a solution

in which the component loadings are highly correlated in all three modes and are therefore highly redundant and difficult to interpret. Degenerate solutions may cause problems with convergence when fitting the model, and usually indicate that the data require a model more general than PARAFAC. Degeneracy can be avoided by constraining the model components in at least one of the three modes to be orthogonal. Although this results in a poorer fit and compromises to some extent the intuitive appeal of the model, an orthogonal solution will generally be more interpretable than the degenerate solution. It should be noted that the inherent uniqueness of the PARAFAC model is not compromised by imposing orthogonality constraints. In this section we examine the effect of orthogonality constraints on the TC model's ability to fit our PVEP data.

Degenerate solutions are easily recognized by the presence of (1) high correlations (roughly greater than 0.8, although the cut-off is arbitrary) in all three modes between the loadings of two or more components and (2) a negative triple product of correlations (A-mode correlation × B-mode correlation × C-mode correlation, with either one or all three of these being negative) between the loadings of those components that are highly correlated. The normalized scalar cross-product between the loadings is an analagous measure of similarity which can be used to look for degeneracy (Lundy and Harshman 1985). It is defined for mode A (and analogously for modes B and C) as follows:

$$C_a(j,k) \triangleq \frac{\sum_{i=1}^{I} a_j(i)\, a_k(i)}{\sqrt{\sum_{i=1}^{I} a_j^2(i) \sum_{i=1}^{I} a_k^2(i)}} \qquad (9)$$

where j and k index the components. Unlike the correlation, the cross-product includes the loadings' constant offsets (means) as well as their dynamics in quantifying their similarity. The cross-product is a more natural measure to use if one thinks of the model components in each mode as vectors whose similarities are determined by the angles between them. Given this interpretation, the cross-product is equal to the cosine of the angle between the vectors. Thus, the cross-product ranges from -1 to +1, and a value of zero means components j and k are orthogonal on the given mode. Constraining a solution to be orthogonal on mode A for example, means forcing $C_a(j,k) = 0 \ \forall \ j,k, \ j \neq k$. It is necessary to impose orthogonality on only one of the three modes to prevent a degenerate solution (Harshman and Lundy 1984a).

In choosing the mode to constrain, one must consider the effect of the constraint on goodness-of-fit as well as on the interpretability of the resulting solution. Below in this section we compare fit-dimensionality curves obtained by fitting the TC model, unconstrained and orthogonally constrained in each of the three modes, to our PVEP data. We also look at an example of the effect that each constraint has on the cross-products of the two unconstrained modes. Our purpose is to get an idea of what to expect in terms of fit and interpretability when using the orthogonally-constrained TC model and, should it be necessary for our data, to select the appropriate mode to constrain.

The data were preprocessed by normalization across subjects and B-centering. The PARAFAC program was used to fit first- through fifth-order models using each of four constraint options: orthogonality in each of the three modes, and unconstrained. The cross-products were used to check for degeneracy.

The third-order model provides a representative example of the results obtained at each of the various dimensionalities. Table I shows the cross-product matrix in each mode for the third-order unconstrained and orthogonal solutions. Extreme degeneracy is indicated for the unconstrained solution: all cross-products are greater than 0.9 in magnitude, and the triple product of the A-, B-, and C-mode cross-products is negative for components 1 vs. 2 (.99 × -1.0 × 1.0) and also for components 1 vs. 3 (.97 × -1.0 × .99). The same pattern of degeneracy resulted from three different starting positions, and solutions at all orders (greater than two) were similarly degenerate. This was a clear indication that an orthogonality constraint would be necessary to obtain an interpretable solution for this data set.

Referring to the cross-product matrices for the orthogonal solutions, note that imposing orthogonality on mode A reduced the extreme similarity between the components in mode C (at least with respect to component 3) and vice versa (although to a lesser degree). Neither A- nor C-mode orthogonality, however, significantly reduced the similarity between components in mode B. This suggests that the similarity between the B-mode (spatial) components was strongly determined by the data; i.e., that imposing orthogonality on mode B is less "natural" for these data than imposing either A- or C-mode orthogonality. The fit-dimensionality curves (Figure 2) support this conclusion: note that B-mode orthogonality is the only constraint that significantly degraded the fit, while the curves corresponding to A- and C-mode orthogonality are almost indistinguishable from the unconstrained curve.

The above observations support two conclusions: (1) Due to the extreme degeneracy of the unconstrained solutions an orthogonality constraint will be necessary to obtain an interpretable solution for this data set. (2) Due to the apparent tendency toward extreme similarity between components in mode B, either A- or C-orthogonal

Table I. Cross-product matrices: third-order solutions. Since these matrices are symmetrical, only the upper triangles are shown. All diagonal entries are 1.0, since any component is maximally similar to itself.

		MODE A			MODE B			MODE C		
		1	2	3	1	2	3	1	2	3
UNCONSTRAINED:	1	1.0	.99	.97	1.0	-1.0	-1.0	1.0	1.0	.99
	2		1.0	.92		1.0	1.0		1.0	.98
	3			1.0			1.0			1.0
A-ORTHOGONAL:	1	1.0	0	0	1.0	.99	-.98	1.0	.80	-.04
	2		1.0	0		1.0	-.96		1.0	-.05
	3			1.0			1.0			1.0
B-ORTHOGONAL:	1	1.0	.93	.48	1.0	0	0	1.0	.96	-.65
	2		1.0	.55		1.0	0		1.0	-.55
	3			1.0			1.0			1.0
C-ORTHOGONAL:	1	1.0	.68	.72	1.0	-.98	.97	1.0	0	0
	2		1.0	.55		1.0	-.99		1.0	0
	3			1.0			1.0			1.0

solutions would be preferable to B-orthogonal solutions for this data set. Both A- and C-orthogonal solutions will therefore be considered when proceeding with the analysis. However, it should be noted that like centering options, orthogonality constraints are data-specific. Experience with the TC model may eventually reveal particular constraints to be appropriate in certain situations.

To conclude this section on orthogonality constraints, we comment that degenerate solutions have been a frequent occurrence in our experience with the TC model, and were quite discouraging initially. Orthogonality constraints, though not very satisfying intuitively in light of their "artificial" quality, have often made the TC model useful when otherwise it would not have been.

Data Reduction: TCA vs. PCA

Before proceeding with the analysis of our PVEP data, we used the data to determine how the TC model compares to traditional principal components (PC's) in terms of data reduction. A multisubject MEP waveform set, though it may be put in the form of a three-way data array and fit with the trilinear TC model, remains a set of waveforms that can as easily be subjected to PCA. (Since any PCA is based on a bilinear model, the PCA must be performed on a two-way, "collapsed" version of the three-way array. See Möcks, 1988a, eqs. 2—3 for two alternative bilinear models that could underly such a PCA.) In using the trilinear TC model, one makes an assumption about the underlying structure of the data that is not required when using a bilinear model: namely, that a given temporal component is associated with a single topographic distribution (spatial component) that is common to all subjects and all sample times. This gives the TC model greater parsimony at the expense of generality. If the additional assumption is reasonable for a given data set, then a greater degree of data reduction should be possible for a given goodness-of-fit using the TC model. If the assumption is inappropriate, the TC model should have difficulty fitting the data, and a more general PC-type model should consequently provide greater data reduction for a given goodness-of-fit (or equivalently, a better fit for a given degree of data reduction). The present analysis was done to determine which would be the case for our PVEP data.

The data were fit with the TC model as defined by eq. (1), and a PC model at first- through fifth-order. At each dimensionality and for each model, the goodness-of-fit was noted and the degree of data reduction computed from the number of parameters in the model and the number of data points. The two models were then compared by plotting the goodness-of-fit against the degree of data reduction. As a check on the validity of this comparison, both models were fit to a random data set which contained no information for which either model could be considered more or less appropriate. Therefore, the two models were expected to be comparable in fitting the random data.

The actual data were preprocessed with A-mode normalization and B-mode centering. The TC model was fit

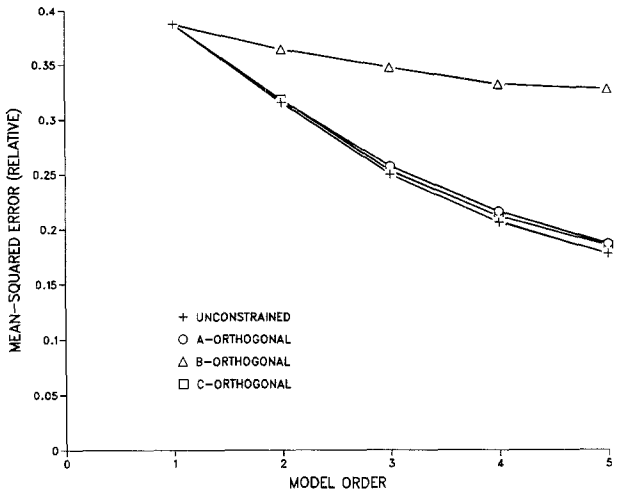

Figure 2. Fit-dimensionality curves show effects of orthogonality constraints.

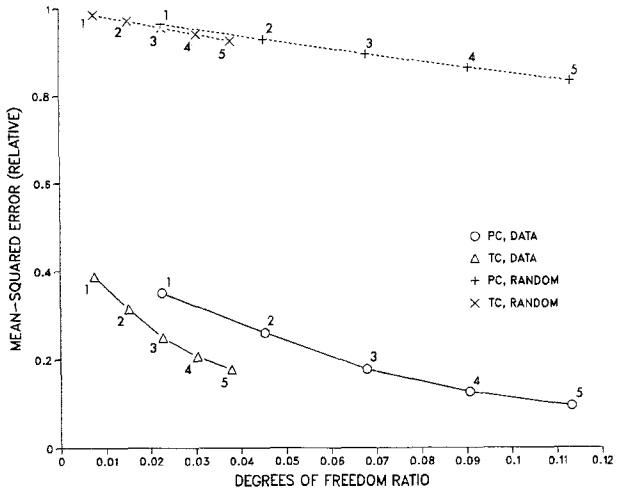

Figure 3. MSE-DFR curves comparing topographic components (TC) with principal components (PC). Solid curves, actual data; dashed curves, random data. Each point is labelled with the order of the model to which it corresponds.

to the 30 × 8 × 64 data array in the same manner as described previously, with no orthogonality constraints. In order to fit a bilinear PC model, the preprocessed data were collapsed into a 240 (= 30 × 8) × 64 matrix such that the PC model would be defined as follows (see Möcks 1988a, eq. 2):

$$x(i,l,t) \approx \sum_{k=1}^{N} b_k(i,l)\, c_k(t) \qquad (10)$$

Pre-multiplication of this matrix by its transpose gave a 64 × 64 cross-product matrix which was subjected to PCA using the singular value decomposition. Note that using the cross-product matrix rather than the more traditional covariance or correlation matrix renders the PCA equivalent to a direct fit of eq.(10) to the preprocessed data. A 30 × 8 × 64 array of standard normal deviates constituted the random data set.

Goodness-of-fit was quantified by the relative MSE. Data reduction was quantified by the degrees of freedom ratio (DFR - Carroll and Chang 1970), defined as the ratio of degrees of freedom for the model (the number of free parameters) to degrees of freedom for the data (the total number of data points minus the number determined by preprocessing). Thus a small DFR corresponds to a high degree of data reduction.

The MSE-DFR curves are shown in Figure 3. There are four curves, since each model was fit to both the actual and random data sets. For the random data set, there is no significant difference between the TC and PC curves, as expected. It is therefore confirmed that the MSE-DFR curves provide a valid comparison of the models' appropriateness and data reducing power for the actual data.

For the actual data the TC curve is everywhere below the PC curve. Therefore for any order PC model there is a TC model, albeit of higher order, which provides a better least-squares fit to the data and a greater degree of data reduction. For example, the second-order PC model fit the data to a MSE of 0.26 with a DFR of 0.045, which is a data reduction of (1 - 0.045) × 100 = 95.5%. The fourth-order TC model fit the data to a MSE of 0.21, with 96.2% data reduction. The difference between 95.5% and 96.2% data reduction is 200 model parameters.

The above result supports the conclusion that for this data set at least, the TC model is superior to the PC model as far as data reduction is concerned. The seemingly restrictive assumption of spatial components common to all subjects and sample times is apparently not inappropriate. Rather, it enables the TC model to exploit additional redundancy in the data and thus represent the data more parsimoniously. Whether the TC model will be appropriate for all stimulus modalities under all conditions, or when the subject group is less homogeneous than in the present example, remains an open question.

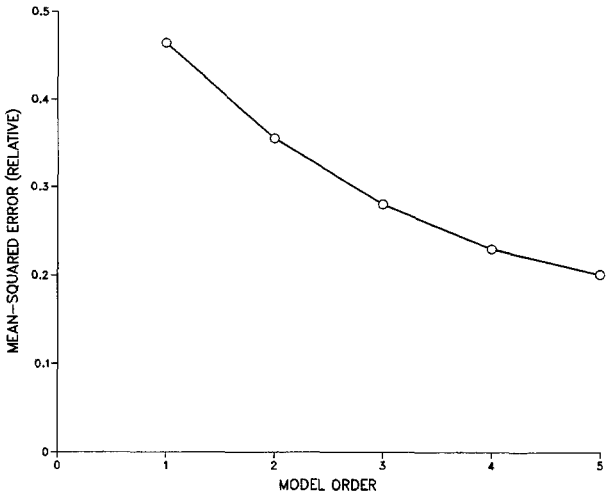

Figure 4. Fit vs. dimensionality for 60-subject data set, A-normalized and B-centered, with no orthogonality constraints. Curves for A- and C-orthogonal solutions not shown are virtually superimposable on the curve shown here.

Topographic Component Analysis of PVEP Data

Identification of Reproducible Solution by Split-Half Analysis

It is clear from the results of the previous section that the TC model can be a powerful data reduction tool for MEP's. An equally important question is whether it can provide a description of the data which is interpretable and meaningful. We now attempt to answer this question for our PVEP data, and try to identify a meaningful set of components to represent the data.

Harshman and Lundy (1984b) recommended confirming that a particular PARAFAC solution is "real" before selecting it for interpretation from among the many possible solutions associated with different combinations of dimensionality, preprocessing method and orthogonality constraint. In other words, an identified set of components should be more than just a least-squares approximation to a particular data set. Ideally, the components will reflect some real phenomena that were measured by, but are unobservable in, the data.

The method used in the present study to "validate" a given solution was to fit the model to random split-halves of the data, making the split across subjects, and to compare components between the two halves (Harshman 1984). The rationale is that a given component would not likely be identified for two different groups of subjects unless it were in some sense meaningful. This may not, however, be a fair test if the sample sizes are too small after splitting the subjects into two groups (Harshman and DeSarbo 1984). Rather than split our thirty-subject data set in half, we combined it with data from an additional thirty subjects, acquired using the same protocol, criteria for normality, etc., as for the original data. Our goal was then to identify a set of components for this sixty-subject, eight-channel, PVEP data which (1) accounted for an adequate proportion of the total data-mean-squares, (2) was not degenerate, and (3) was reproducible to a good approximation in random split-halves of thirty subjects each. (Actually, three subjects were deemed outliers and excluded from the split-halves.)

With both A- and C-orthogonal solutions under consideration, it remained to choose between the two constraints and also to select the order of the model. The first step taken was to fit the TC model at orders one through five to the sixty-subject data (A-normalized and B-centered), using three different constraint options: (1) A-orthogonal, (2) C-orthogonal, and (3) unconstrained. The results of these initial fittings of the model led to four noteworthy observations:

1. The fit-dimensionality curves for both the A- and C-orthogonal solutions (Figure 4) are virtually superimposable on the unconstrained curve, as was the case for the thirty-subject data (Figure 2).

2. The fit-dimensionality curve has no apparent "elbow" that would suggest a "correct" dimensionality. However, by estimating the SNR for the data, a rough idea of what dimensionality to expect could be obtained: typical peak-to-peak amplitudes are 50 μV for the background EEG and 15 μV for the EP. Two-hundred trials were averaged, so the expected SNR would be $(15/50)\sqrt{200} = 4.2$. However, this estimate is based on an idealized concept of signal averaging, so it should be considered an upper bound. Moreover, the effect of data centering on the SNR, as noted previously, is to reduce it - by how much is uncertain. Finally, no theoretical model can be expected to account for all of the true signal variance. Given these considerations it was assumed that the effective SNR was between three and four, so that a relative MSE of roughly 0.20-0.25 was expected. Initial consideration was limited to solutions of dimensionalities three to five, at which the model gave MSE's of 0.28, 0.23, and 0.20, respectively (Figure 4).

3. All solutions (of dimensionality two and higher) were highly degenerate, indicating the need for an orthogonality constraint. Based on results presented earlier we considered constraints only on modes A and C.

Table II. Comparison of split-half solutions (PQ vs. RS) by cross-products in modes B and C: third-order, C-orthogonal solutions.
*With the components matched this way, RI = $[(1.0)(.85)(1.0)(.91)(.99)(.75)]^{1/6}$= .91.

	MODE B			MODE C		
PQ:	1	2	3	1	2	3
RS: 1	1.0*	-.97	-1.0	.85*	-.07	-.50
2	-.98	1.0*	.98	.06	.91*	.07
3	-.99	.99	.99*	.42	-.18	.75*

4. Three of the 60 subjects appeared to be outliers in that the MSE's for their data were consistently higher (by more than 2.5 standard deviations) than the MSE's for the other subjects' data. These subjects' data were retained in the complete data set but excluded from the split-halves, where their influence might have been inflated by the small sample sizes to the point of preventing a good solution from being reproduced in each split-half.

The remaining 57 subjects were divided by the following split-half technique (Harshman 1984) to guard against an "unlucky" split: the subjects were randomly assigned to four groups (three getting 14 subjects, one getting 15) named P, Q, R, and S. These groups were then paired two ways: PQ-RS and PS-QR. The TC model was fit separately to the subsets PQ, RS, PS, and QR, and solutions were compared between the PQ-RS halves and between the PS-QR halves. Any component that replicates across either of these split-half pairs, neither of which shares any common subjects, can be considered meaningful (Harshman 1984).

Six "versions" of the TC model were tested for reproducibility of components across split-halves: A-orthogonal solutions at dimensionalities from three to five, and C-orthogonal solutions likewise. Comparisons between components across split-halves were based on the cross-products between the B- and C-mode loadings of corresponding components. There is no reason to have compared the A-mode loadings since they are subject-dependent; i.e., it is only the spatial and temporal components that we hope to reproduce. The CMPARE routine in the PARAFAC analysis package was used to compute the cross-products for all possible pairings of components across split-halves. Note that the cross-products used to compare components across split-halves are defined just as in eq. (9), only here the jth and kth components come from different solutions.

It was not always obvious from the cross-products which components corresponded between the split-half solutions - some criterion for matching up the components was needed. The PARAFAC convention for sequencing the components is often inadequate for this purpose. The objective for this study was to identify the one solution that could be considered the most meaningful based on overall reproducibility of components, both spatial and temporal, across split-halves. A solution for which all components replicated reasonably well was preferred to a solution for which one or two components replicated extremely well and the rest not well at all. Therefore, the components were matched so as to maximize an overall reproducibility index (RI):

$$RI \triangleq \left[\prod_{k=1}^{N} \sqrt{C_b(p_k)\ C_c(p_k)} \right]^{\frac{1}{N}} \tag{11}$$

where each p is a pair of pointers to the components being matched, for example,

$$p_1, p_2, p_3 = (1,1), (2,3), (3,2) \tag{12}$$

and where C_b (p_k) and C_c (p_k) are the B- and C-mode cross-products respectively for the pair of components indicated by p_k. The RI is simply the geometric mean of all $2N$ cross-products (one in mode B and one in mode C, for each pair of components) for a given choice of component pairings. It therefore ranges from -1 to +1, as do the cross-products themselves. The RI served as the criterion used to match the components and to select the most reproducible solution from the six considered.

Table II shows an example of how the B- and C-mode components are compared between split-halves by cross-products and then matched. These cross-product matrices compare the third-order, C-orthogonal solutions fit to split-halves PQ and RS. Corresponding components, as determined by maximizing the RI, are indicated. They happen to be on the diagonal in this case, i.e., corresponding components have the same sequence position in the solutions being compared - this does not always occur. The RI for the optimal pairings as shown is computed as the geometric mean of the indicated cross-products,

$$RI = [(1.0)(.85)(1.0)(.91)(.99)(.75)]^{1/6} = 0.91 \tag{13}$$

The third-order, C-orthogonal solution gave the highest RI among the six solutions, as shown in Table III. Each RI listed is the better of two, one for PQ-RS and one for PS-QR.

Table III. Best reproducibility indices for six solutions.

	ORTHOGONALITY	
N	MODE A	MODE C
3	.86	.91
4	.80	.82
5	.77	82

An RI of 0.91 indicates a high degree of overall similarity between both the temporal and spatial components of the split-half solutions. This is important because it indicates that the TC model is effecting a unique, meaningful decomposition of the data – for if the model provided nothing more than an arbitrary least-squares approximation, a given set of components would not likely be reproduced in different subjects. This is not to say that the components necessarily correspond to the physical sources that generated the data. The components do, however, have an empirical validity that an arbitrarily rotated set of principal components could not have.

Note that the reproducibility of components suggests the possibility of generalizing a set of components, identified for a particular group of subjects, to new subjects not part of the group. For example, one can envision using the TC model to reduce an MEP data base, consisting of data from a large number of subjects in a given diagnostic group, to a set of spatial and temporal components characteristic of the group. Once this were done for various groups, new subjects could be compared to each group by determining how well and in what proportions a group's components predict the subject's MEP data. This would involve computing a set of subject scores for the new subject, which is easily done by multiple regression of the subject's data onto the components identified for the group. A statistical comparison could then be based on the subject scores alone. The reader is referred to Field (1991, Chapter 5) for further discussion and a demonstration of this approach.

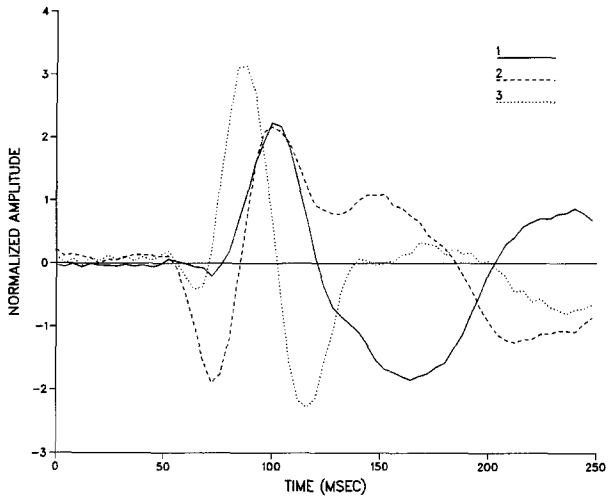

Figure 5. Temporal components for 60-subject data set: third-order, C-orthogonal solution.

Examination of TC Model Solution

In the previous section it was found that among the six solutions considered, the third-order, C-orthogonal solution was the most reproducible in split-halves of the data. The same components identified for the split-halves were expected to be identified for the complete sixty-subject set, and indeed they were: RI's of 0.97 were obtained when the sixty-subject solution was compared to solutions for split-halves PQ and RS. Thus, virtually the same set of components was identified for the complete data set as for the split-halves. It was then concluded that the third-order, C-orthogonal solution is indeed the best solution among those those considered for the sixty-subject, eight-channel PVEP data, and this solution will now be examined.

The temporal components are plotted in Figure 5, the spatial component loadings are listed in Table IV. A histogram of subject scores was constructed for each component, shown in Figures 6(a-c). Figure 7 shows the

Table IV. Spatial component loadings for sixty-subject data set: third-order, C-orthogonal solution. Loadings are positioned in the table according to scalp locations, as shown at the left.

LOCATIONS			COMPONENT 1			COMPONENT 2			COMPONENT 3		
C3	Cz	C4	-.88	-1.1	-.85	-.89	-.85	-.98	-.95	-1.0	-.96
P3	Pz	P4	-.12	-.25	.04	-.30	.03	-.25	-.19	-.02	-.01
O1		O2	1.5		1.7	1.3		1.9	1.4		1.8

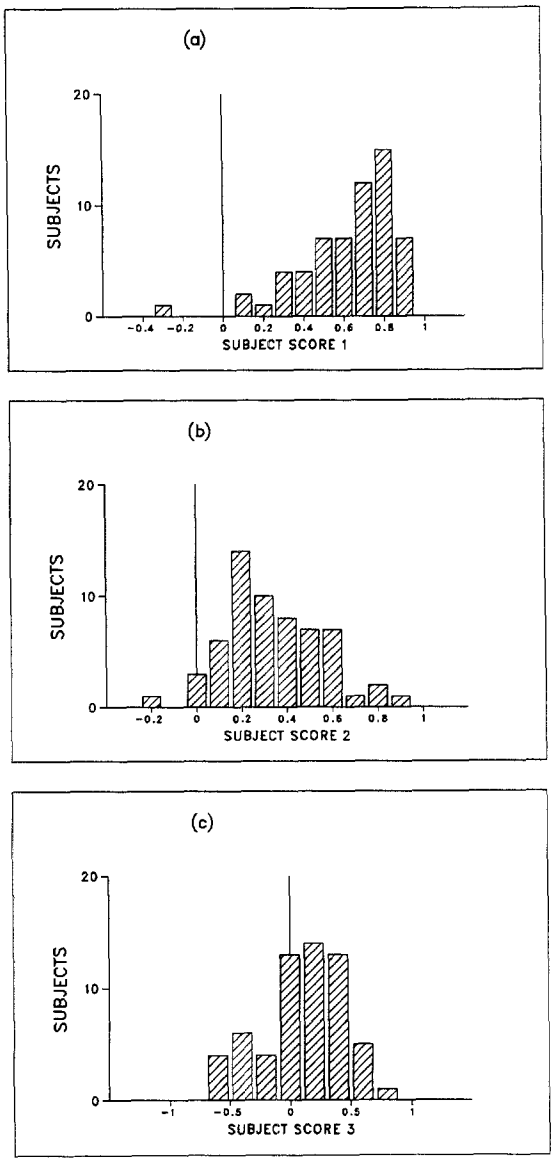

Figure 6. Subject-score histograms for 60-subject data set: third-order, C-orthogonal solution (a-c, components 1-3, respectively).

data waveforms averaged over subjects for each location. Note that the third-order, C-orthogonal solution fit the sixty-subject data to a relative MSE of 0.28.

The temporal and spatial components as shown in Figure 5 and Table IV are normalized such that the subject scores reflect the scale of the data, although the data were normalized such that all subjects have a mean-square equal to one. The sign convention adopted was to minimize the number of negative A-mode loadings (subject scores), which have an artificial quality to them. The same would be true of the B-mode loadings, were the data not centered on mode B (Field and Graupe 1990a). With B-centering, however, both positive and negative

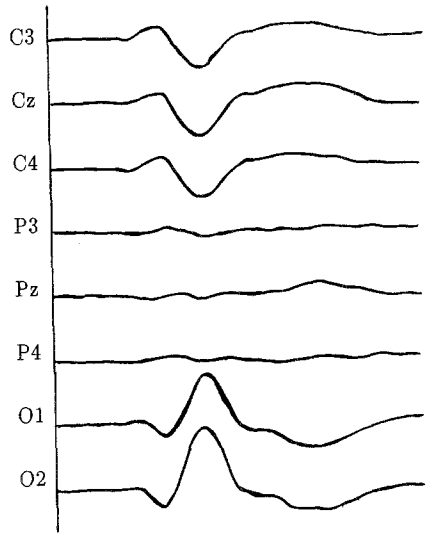

Figure 7. Mean EP waveforms by scalp location, for the 60 subjects.

loadings are inevitable. There is no theoretical basis for choosing the signs of the B- and C-mode loadings once the signs of the A-mode loadings have been fixed. Their signs can therefore be considered arbitrary; i.e., the polarity of a given temporal component can be changed, provided the polarity of the associated spatial component is also changed.

The sequence convention used by the PARAFAC algorithm is to order the components by decreasing "RMS contribution," which is defined as

$$RMS_k \triangleq \sqrt{\frac{1}{ILT} \sum_{i,l,t} a_k^2(i)\ b_k^2(l)\ c_k^2(t)} \tag{14}$$

where RMS_k is the RMS contributon of the kth component to the predicted data. Note, in Field and Graupe (1990a) we defined the component "magnitude" G_k by treating the set of loadings in each mode as a vector, and taking the triple-product of the three vector magnitudes. The relationship between G_k and RMS_k is

$$G_k \equiv RMS_k \sqrt{ILT} \tag{15}$$

i.e., they are equivalent measures differing only by a constant.

Looking first at the mean waveforms (Figure 7), note that the central electrodes (C3, Cz, C4) show opposite polarity to the occipital electrodes (O1, O2), and the

parietal electrodes (P3, Pz, P4) show very low signal levels. This configuration suggests that the post-centering zero-potential lines tend to traverse the scalp coronally in the vicinity of the parietal electrodes.

The spatial components (Table IV) are all quite similar and generally consistent with the appearance of the mean waveforms, in that all are positive occipitally and negative centrally, with smaller loadings at the parietal locations. That the spatial components would be so similar was not unexpected. Recall that similarity among components in mode B was highly determined by the data. There are subtle differences between the spatial components, e.g., components 1 and 3 have maximum negativity at the vertex (Cz), while component 2 is more negative bilaterally. Such features are difficult to interpret without examining the topographies present in the data for individual subjects and sample times. No attempt to do so will be made here – rather, we turn our attention to the temporal components.

The first temporal component (Figure 5) resembles the mean waveforms (Figure 7), those at O1 and O2 being the most obvious comparisons given the chosen polarity of the components. This is no surprise, since the data were not centered on the subject mode; i.e., the mean waveforms shown in Figure 7 were not subtracted from the data. Thus, the best one-component description of the data, insofar as the time mode is concerned, would be the grand mean waveform, or the average of the eight mean waveforms shown.

The second temporal component shows marked peaks at approximately 75 and 100 msec, negative and positive, respectively. Peaks at these latencies and polarities are typical of PVEP waveforms and are usually referred to as N75 and P100. The third temporal component is difficult to interpret at a glance, but a closer look reveals that component 3 looks like the time-derivative of component 2, up to approximately 120 msec. This is an important observation because any signal and its time-derivative constitute the first two terms of the Taylor's-series expansion for a time-shifted version of the signal, when the derivative is weighted by the amount of shift:

$$c(t \pm \tau) \approx c(t) \pm \tau \frac{dc(t)}{dt} \qquad (16)$$

Thus, variously weighted sums of temporal components 2 and 3 will approximate various time-shifted versions of component 2, i.e., component 2 with various latencies. The fitting algorithm apparently "recognized" that the data required various time-shifted versions of a given component for a proper fit, and produced the component along with its time-derivative to achieve an approximation of that ideal. Indeed, this has been demonstrated to occur in simulation studies with PCA, using data synthesized from variable-latency components (Möcks 1986). It was hypothesized at this point that the third component is an "artificial" one that resulted, at least in part, from the need to explain the variability of P100 latencies seen in normal subjects. This result will be studied more closely after examining the subject scores (Figure 6).

First, note that if the subject scores were to be used in any statistical analyses, the assumption that they are normally distributed would be poor, at least for component 1. A transformation to achieve approximate normality would be useful in this regard. Fisher's Z-transformation for correlation coefficients might be appropriate since, given the present combination of preprocessing and orthogonality constraint, each subject score is indeed the coefficient of correlation between a given subject's data values and a given component (Harshman and Lundy 1984b). Also note that for each of the first two components, only one subject score is significantly less than zero. A large number of negative subject scores would constitute evidence against the physiologic reality of a given component, though the converse is not true.

In contrast to the first two components, many subject scores on component 3 are negative (further evidence of the "artificiality" of this component). This means that for these subjects the second and third temporal components, with the polarities as shown in Figure 5, are differenced rather than summed. This is true because (1) the component-2 subject scores are all positive, and (2) the second and third spatial components have like signs at all locations. From eq. (16), when temporal components 2 and 3 are differenced they will approximate a time-delayed version of component 2, i.e., component 2 with an extended latency. For those subjects whose third subject score is positive, such that components 2 and 3 are summed, these components will approximate a time-advanced version of component 2, or component 2 with a shortened latency.

It is clear that the first two temporal components with their peaks at 100 msec serve to explain the P100 peaks in the data that occur at or very near the average latency of 100 msec. Now with the above result, we have evidence that component 3 is acting at least in part to approximately shift component 2 to the left or right as necessary to account for P100 peaks occurring significantly before or after 100 msec. A simple test of this hypothesis was performed as described below.

If the above-mentioned hypothesis is true, then by eq. (16), the amount of shift applied to component 2 should be proportional to the relative weight of component 3. Therefore, subject scores on component 3, which by definition represent the relative weights of component 3, should contain information about P100 peak latencies.

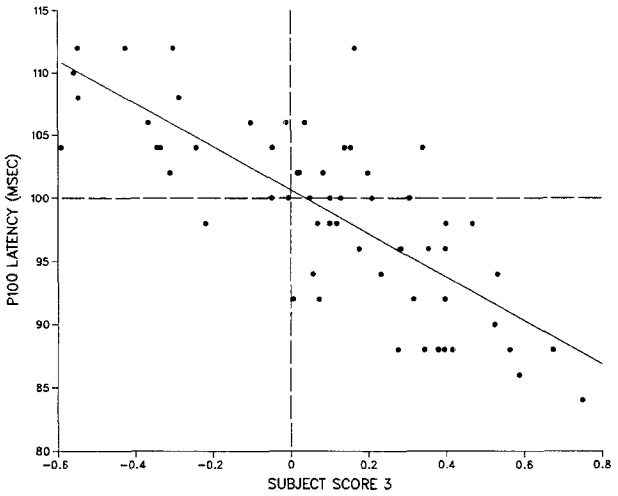

Figure 8. P100 peak latencies measured on the data (60 subjects) vs. subject scores on component 3, with fitted regression line (r = -0.775).

To confirm or deny this, correlation was sought between P100 latency and third subject score for all 60 subjects. Peak latencies were crudely measured as the time of maximum potential between 80 and 120 msec for the sampled data (4 msec sampling period resulting in ±2 msec precision)-hardly a robust method in the face of noise and ill-defined peaks, not to mention the sampling error, but adequate for the present purpose. P100 latency was taken to be the average of latencies measured for channels O1 and O2, the two locations with the strongest signals.

The correlation coefficient was found to be r=-0.775, which confirms that subject scores on the third component indeed contain information about actual P100 latencies in the data. Had peak latencies been measured more carefully, the correlation would likely be somewhat stronger. The latency/subject-score data are scatterplotted in Figure 8 along with a standard regression line. Note that the y-intercept of the regression line is approximately 100 msec, the expected latency of the P100 peak. This supports the conclusion that for a given subject, the third component tended to be weighted in proportion to the time-difference between expected and actual P100 latency.

Only one data set was analyzed and, with regard to the latency question, the focus was on only one waveform peak (P100). In practice, the situation is surely not as simple as that described here. Other waveform features must come into play, as must topographic features which were not considered. Moreover, an obvious component/derivative relationship such as observed between the second and third components is hardly guaranteed to occur every time latency variations are present. Nevertheless, that such a relationship was identified in the analysis of actual data lends much support to the conclusion reached by Möcks (1986) in his PCA simulation studies, and extends that conclusion to TC analysis: namely, that it might be fruitful to somehow explicitly incorporate component time-derivatives into the PC and TC models, in order to make these models more appropriate for data containing significant latency variations.

We make one final point regarding the significance of the above result as depicted in Figure 8: it suggests a new aspect to the analysis of subject scores. The scores would normally be thought of as simply the relative contributions of the components to the data, and they are indeed just that. Now, though, we have a clear example of subject scores providing direct information about peak latencies in the data. Given the important role of peak latencies in clinical diagnosis, this result could have significance to the statistical analysis of TC (or PC) model subject scores (e.g., for classification purposes, as in Field 1991; see also Field and Graupe 1990b).

Concluding Remarks

The TC/PARAFAC model provides a theoretically unique spatiotemporal decomposition of multichannel evoked potentials recorded from a group of subjects. Proper application of the model requires careful preprocessing of the data, recognition of degenerate solutions, judicious use of optional orthogonality constraints, selection of appropriate model order, and validation of solutions. This is difficult to accomplish blindly, with no theoretical basis for making the required decisions or knowledge of what results to expect from them. It is impossible to consider every combination for a given application. This paper provides theoretical and empirical guidelines for these procedures in the context of MEP's, along with a specific exemplified approach to the required decision-making process. This approach was used successfully to obtain for the first time a unique, meaningful and reproducible spatiotemporal (trilinear) decomposition of an actual MEP data set. In so doing, the appropriateness of the model and the practicability of the method to MEP's were clearly established for the first time.

Although these preliminary results are encouraging, it must be emphasized that only a single, fairly homogeneous data set, of MEP's for only 8 channels and for a single stimulus modality, was analyzed. Further study is required to assess the appropriateness of the TC model for a variety of stimulus modalities, experimental conditions, existing pathologies, etc. Hopefully, future

studies will also ascertain under what circumstances particular preprocessing and/or orthogonality constraints are most appropriate, obviating the need to make a decision on these options with each application of the model. Taking this a step further, it should be possible to identify sets of spatial and temporal components that summarize large MEP data bases from various diagnostic groups, as well as from the normal population. Once these components are available, the MEP's of new subjects can be compared to each group by a simple calculation of subject scores only, with no need for a complete TC analysis (see Field 1991, Chapter 5).

Another area for future work concerns the problem of latency jitter. Our demonstration of the effects of latency jitter on the TC model solution lends support to the idea originally suggested for PCA (Möcks 1986), of explicitly incorporating time-derivatives into the model in the form of additional components. Another possibility is to apply a time-warping technique to the data as a preprocessing step. Time-warping is common in speech processing (see Rabiner and Schafer 1978), and the rationale for its application to MEP's would be the same: namely, that minor compressions and dilations of the time axis do not change the essential information contained in the signal; rather they allow meaningful comparisons between sampled signals by bringing significant events into temporal alignment. Using time-warping to align major EP waveform peaks might make the TC decomposition more meaningful by removing arbitrary and irrelevant time-scale differences between subjects. Of course, latency variations may not be irrelevant, and they would remain available for analysis in a separated form by virtue of the warping functions.

As a final note, it should be reemphasized that no fixed "recipe" for TC analysis is possible or even desirable. The TC model is simply another potentially very powerful analysis tool at our disposal that must be used with good judgement. It is hoped that this current work will serve as a foundation for future studies of the TC model, and provide helpful guidance to those who pursue this new approach to MEP analysis.

References

Bio-logic Systems Corp. Guidelines for Normative Data Collection: Brain Atlas Systems. Mundelein, Illinois, July 1988.

Carroll, J. D. and Chang, J. J. Analysis of individual differences in multidimensional scaling via an N-way generalization of "Eckart-Young" decomposition. Psychometrika, 1970, 35:283-319.

Carroll, J. D. and Pruzansky, S. The CANDECOMP-CANDELINC family of models and methods for multidimensional data analysis. In: Law, H. G., Snyder, Jr., C. W., Hattie, J. A., and McDonald, R. P. (eds.), Research Methods for Multimode Data Analysis, Praeger, New York, 1984: 372-402.

Donchin, E. and Heffley, E. F. Multivariate analysis of event-related potential data: A tutorial review. In: Otto, D. A. (ed.), Multidisciplinary Perspectives in Event-Related Brain Potential Research, U.S. Gov. Printing Office, Washington, DC, 1978: 555-572.

Field, A. S. Applied Topographic Component / Parallel Factor Analysis for Spatiotemporal Decomposition of Multichannel Evoked Potentials. Ph.D. thesis, Department of Bioengineering, University of Illinois at Chicago, 1991.

Field, A. S. and Graupe, D. Topographic components analysis of evoked potentials: Estimation of model parameters and evaluation of parameter uniqueness. J. Biomed. Eng., 1990a, 12:287-300.

Field, A. S. and Graupe, D. Topographic components analysis of evoked potentials: Parameter estimation and some preliminary results. Proc. IEEE Int. Symp. Circ. Syst. (ISCAS), New Orleans, 1990b: 2049-2052.

Glaser, E. M. and Ruchkin, D. S. Principles of Neurobiological Signal Analysis. Academic Press, New York, 1976: 233-290.

Harner, R. N. Singular value decomposition-A general linear model for analysis of multivariate structure in the electroencephalogram. Brain Topography, 1990, 3:43-47.

Harshman, R. A. Foundations of the PARAFAC procedure: Models and conditions for an 'explanatory' multi-modal factor analysis. UCLA Working Papers in Phonetics (University Microfilms #10,085), 1970, 16:1-84.

Harshman, R. A. 'How can I know if it's "real?"' A catalog of diagnostics for use with three-mode factor analysis and multidimensional scaling. In: Law, H. G., Snyder, Jr., C. W., Hattie, J. A., and McDonald, R. P. (eds.), Research Methods for Multimode Data Analysis, Praeger, New York, 1984: 566-591.

Harshman, R. A. and De Sarbo, W. S. An application of PARAFAC to a small sample problem, demonstrating preprocessing, orthogonality constraints, and split-half diagnostic techniques. In: Law, H. G., Snyder, Jr., C. W., Hattie, J. A., and McDonald, R. P. (eds.), Research Methods for Multimode Data Analysis, Praeger, New York, 1984, 602-642.

Harshman, R. A. and Lundy, M. E. Data preprocessing and the extended PARAFAC model. In: Law, H. G., Snyder, Jr., C. W., Hattie, J. A., and McDonald, R. P. (eds.), Research Methods for Multimode Data Analysis, Praeger, New York, 1984a: 216-281.

Harshman, R. A. and Lundy, M. E. The PARAFAC model for three-way factor analysis and multidimensional scaling. In: Law, H. G., Snyder, Jr., C. W., Hattie, J. A., and McDonald, R. P. (eds.), Research Methods for Multimode Data Analysis, Praeger, New York, 1984b: 123-215.

Lehmann, D. Principles of spatial analysis. In: Gevins, A. S. and Remond, A. (eds.), Methods of Analysis of Brain Electrical and Magnetic Signals, volume 1 of Handbook of Electroencephalography and Clinical Neurophysiology (Revised Series), Elsevier, Amsterdam, 1987: 309-354.

Lundy, M. E. and Harshman, R. A. Reference Manual for the PARAFAC Analysis Package. Scientific Software Associates, London, Ontario, Canada, 1985.

Möcks, J. The influence of latency jitter in principal component analysis of event-related potentials. Psychophysiol., 1986,

23:480-484.

Möcks, J. Decomposing event-related potentials: A new topographic components model. Biol. Psychol., 1988a, 26:199-215.

Möcks, J. Topographic components model for event-related potentials and some biophysical considerations. IEEE Trans. Biomed. Eng., 1988b, 35:482-484.

Möcks, J. and Verleger, R. Principal component analysis of event-related potentials: A note on misallocation of variance. Electroenceph. Clin. Neurophysiol., 1986, 65:393-398.

Nunez, P. L. Electric Fields of the Brain. Oxford Univ. Press, New York, 1981: 22-24.

Offner, F. F. The EEG as potential mapping: The value of the average monopolar reference. Electroenceph. Clin. Neurophysiol., 1950, 2:215-216.

Rabiner, L. R. and Schafer, R. W. Digital Processing of Speech Signals. Prentice-Hall, New Jersey, 1978: 480-484.

Skrandies, W. Data reduction of multichannel fields: Global field power and principal component analysis. Brain Topography, 1989, 2:73-80.

Skrandies, W. and Lehmann, D. Spatial principal components of multichannel maps evoked by lateral visual half-field stimuli. Electroenceph. Clin. Neurophysiol., 1982, 54:662-667.

Wood, C. C. and McCarthy, G. Principal component analysis of event-related potentials: Simulation studies demonstrate misallocation of variance across components. Electroenceph. Clin. Neurophysiol., 1984, 59:249-260.